



High order finite difference WENO schemes with the exact conservation property for the shallow water equations[☆]

Yulong Xing^a, Chi-Wang Shu^{b,*}

^a *Department of Mathematics, Brown University, Providence, RI 02912, United States*

^b *Division of Applied Mathematics, Brown University, Providence, RI 02912, United States*

Received 27 July 2004; received in revised form 3 December 2004; accepted 13 February 2005

Available online 13 April 2005

Abstract

Shallow water equations with nonflat bottom have steady state solutions in which the flux gradients are nonzero but exactly balanced by the source term. It is a challenge to design genuinely high order accurate numerical schemes which preserve exactly these steady state solutions. In this paper we design high order finite difference WENO schemes to this system with such exact conservation property (C-property) and at the same time maintaining genuine high order accuracy. Extensive one and two dimensional simulations are performed to verify high order accuracy, the exact C-property, and good resolution for smooth and discontinuous solutions.

© 2005 Elsevier Inc. All rights reserved.

Keywords: Shallow water equation; WENO scheme; High order accuracy; Source term; Conservation laws; C-property

1. Introduction

The shallow water equations, also referred to as the Saint-Venant system, are widely used to model flows in rivers and coastal areas. It has wide applications in ocean and hydraulic engineering: tidal flows in estuary and coastal water region; bore wave propagation; and river, reservoir, and open channel flows, among others. This system describes the flow as a conservation law with additional source terms. We consider the system with a geometrical source term due to the bottom topology. In one space dimension, it takes the form

[☆] Research supported by ARO grants DAAD19-00-1-0405 and W911NF-04-1-0291, NSF grant DMS-0207451 and AFOSR grant F49620-02-1-0113.

* Corresponding author. Tel.: +1 401 863 2549; fax: +1 401 863 1355.

E-mail addresses: xing@dam.brown.edu (Y. Xing), shu@dam.brown.edu (C.-W. Shu).

$$\begin{aligned} h_t + (hu)_x &= 0, \\ (hu)_t + \left(hu^2 + \frac{1}{2}gh^2 \right)_x &= -ghb_x, \end{aligned} \quad (1.1)$$

where h denotes the water height, u is the velocity of the fluid, $b(x)$ represents the bottom topography and g is the gravitational constant. In the homogeneous case, the system is equivalent to that of the isentropic Euler system. However, the properties of the system change a lot due to the presence of the source term. The above system is quite simple in the sense that only the topography of the bottom is taken into account, but other terms could also be added in order to include effects such as friction on the bottom and on the surface as well as variations of the channel width.

Research on numerical methods for the solution of the shallow water system has attracted much attention in the past two decades. Many numerical schemes have been developed to solve this system. Similar to other balance laws, this system admits stationary solutions in which nonzero flux gradients are exactly balanced by the source terms in the steady state case. Such cases, along with their perturbations, are very difficult to capture numerically. A straightforward treatment of the source terms will fail to preserve this balance.

A significant result in computing such solutions is given by Bermudez and Vazquez [2]. They have proposed the idea of the “exact C-property”, which means that the scheme is “exact” when applied to the stationary case $h + b = \text{constant}$ and $hu = 0$. This property is necessary for maintaining the above balance. A good scheme for shallow water system should satisfy this property. Also, they have introduced the Q-scheme and the idea of source term upwinding. LeVeque [12] has introduced a quasi-steady wave propagation algorithm. A Riemann problem is introduced in the center of each grid cell such that the flux difference exactly cancels the source term. Zhou et al. [24] use the surface gradient method for the treatment of the source terms. They use $h + b$ for the reconstruction instead of using h . Russo [16] and Kurganov and Levy [11] apply finite volume central-upwind schemes to this system, keeping higher order accuracy for the flux term and second order accuracy for the source term. Recently, Vukovic and Sopta [21] have used the essentially nonoscillatory (ENO) and weighted ENO (WENO) schemes for this problem. They applied WENO reconstruction not only to the flux but also to a combination of the flux and the source term. For related work, see also [10,14,23,8,7,6].

Most of the works mentioned above are for numerical schemes of at most second order accuracy. There is a fundamental difficulty in maintaining genuine high order accuracy for the general solutions and at the same time achieving the exact C-property. The work mentioned above which addresses this issue is [21], see also [22,3]. The schemes in [21,22] are high order accurate for solutions of certain specific forms, but seem to be still only second order accurate for the general solutions based on truncation error analysis. The main objective of this paper is to design a WENO finite difference scheme which maintains the exact C-property and at the same time is genuinely high order accurate for the general solutions of the shallow water equations, via a special splitting of the source term into two parts which are discretized separately. For a related work using a different idea, see [4]. The specific WENO scheme we use is the fifth order finite difference scheme introduced by Jiang and Shu [9]. It uses a convex combination of three candidate stencils, each producing a third order accurate flux, to obtain fifth order accuracy and an essentially nonoscillatory shock transition. Time discretization can be implemented by the TVD Range–Kutta method [18]. For more details of WENO schemes, we refer to [9,17].

This paper is organized as follows. In Section 2, we give a brief review of the finite difference WENO schemes for the homogeneous conservation laws. The WENO scheme which maintains the exact C-property and at the same time is genuinely high order accurate for the general solutions of the shallow water equations is presented in Section 3. Sections 4 and 5 contain extensive numerical simulation results to demonstrate the behavior of our WENO schemes for one and two dimensional shallow water equations,

verifying high order accuracy, the exact C-property, and good resolution for smooth and discontinuous solutions. Concluding remarks are given in Section 6.

2. A review of high order finite difference WENO schemes

In this section we give a short overview of the finite difference WENO schemes. For more details, we refer to [13,9,1,17–19].

First, we consider a scalar hyperbolic conservation law equation in one dimension

$$u_t + f(u)_x = 0$$

with a positive wind direction $f'(u) \geq 0$. For a finite difference scheme, we evolve the point values u_i at mesh points x_i in time. We assume the mesh is uniform with mesh size Δx for simplicity. The spatial derivative $f(u)_x$ is approximated by a conservative flux difference

$$f(u)_x|_{x=x_i} \approx \frac{1}{\Delta x} (\hat{f}_{i+\frac{1}{2}} - \hat{f}_{i-\frac{1}{2}}). \quad (2.1)$$

The numerical flux $\hat{f}_{i+\frac{1}{2}}$ is computed through the neighboring point values $f_j = f(u_j)$. For a $(2k - 1)$ th order WENO scheme, we first compute k numerical fluxes

$$\hat{f}_{i+\frac{1}{2}}^{(r)} = \sum_{j=0}^{k-1} c_{rj} f_{i-r+j}, \quad r = 0, \dots, k-1,$$

corresponding to k different candidate stencils $S_r(i) = \{x_{i-r}, \dots, x_{i-r+k-1}\}$, $r = 0, \dots, k-1$. Each of these k numerical fluxes is k th order accurate. For example, when $k = 3$ (fifth order WENO scheme), the three third order accurate numerical fluxes are given by

$$\hat{f}_{i+1/2}^{(0)} = \frac{1}{3}f_i + \frac{5}{6}f_{i+1} - \frac{1}{6}f_{i+2},$$

$$\hat{f}_{i+1/2}^{(1)} = -\frac{1}{6}f_{i-1} + \frac{5}{6}f_i + \frac{1}{3}f_{i+1},$$

$$\hat{f}_{i+1/2}^{(2)} = \frac{1}{3}f_{i-2} - \frac{7}{6}f_{i-1} + \frac{11}{6}f_i.$$

The $(2k - 1)$ th order WENO flux is a convex combination of all these k numerical fluxes

$$\hat{f}_{i+\frac{1}{2}} = \sum_{r=0}^{k-1} w_r \hat{f}_{i+\frac{1}{2}}^{(r)}.$$

The nonlinear weights w_r satisfy $w_r \geq 0$, $\sum_{r=0}^{k-1} w_r = 1$, and are defined in the following way:

$$w_r = \frac{\alpha_r}{\sum_{s=0}^{k-1} \alpha_s}, \quad \alpha_r = \frac{d_r}{(\varepsilon + \beta_r)^2}. \quad (2.2)$$

Here d_r are the linear weights which yield $(2k - 1)$ th order accuracy, β_r are the so-called ‘‘smoothness indicators’’ of the stencil $S_r(i)$ which measure the smoothness of the function $f(u(x))$ in the stencil. ε is a small constant used to avoid the denominator to become zero and is typically taken as 10^{-6} . For example, when $k = 3$ (fifth order WENO scheme), the linear weights are given by

$$d_0 = \frac{3}{10}, \quad d_1 = \frac{3}{5}, \quad d_2 = \frac{1}{10},$$

and the smoothness indicators are given by

$$\beta_0 = \frac{13}{12}(f_i - 2f_{i+1} + f_{i+2})^2 + \frac{1}{4}(3f_i - 4f_{i+1} + f_{i+2})^2,$$

$$\beta_1 = \frac{13}{12}(f_{i-1} - 2f_i + f_{i+1})^2 + \frac{1}{4}(f_{i-1} - f_{i+1})^2,$$

$$\beta_2 = \frac{13}{12}(f_{i-2} - 2f_{i-1} + f_i)^2 + \frac{1}{4}(f_{i-2} - 4f_{i-1} + 3f_i)^2.$$

The procedure for the case with $f'(u) \leq 0$ is mirror symmetric with respect to $i + \frac{1}{2}$. More details can be found in [9,17].

An upwinding mechanism, essential for the stability of the scheme, can be realized by a global “flux splitting”. The simplest one is the Lax–Friedrichs splitting:

$$f^\pm(u) = \frac{1}{2}(f(u) \pm \alpha u), \tag{2.3}$$

where α is taken as $\alpha = \max_u |f'(u)|$. The WENO procedure is applied to f^\pm individually with upwind biased stencils. Depending on whether the max is taken globally (along the line of computation) or locally, such schemes are referred to as the Lax–Friedrichs WENO scheme (WENO-LF) or the local Lax–Friedrichs WENO scheme (WENO-LLF).

For hyperbolic systems such as the shallow water equations, we use the local characteristic decomposition, which is more robust than a component by component version. First, we compute an average state $u_{i+\frac{1}{2}}$ between u_i and u_{i+1} , using either the simple arithmetic mean or a Roe’s average [15]. The right eigenvectors r_m and the left eigenvectors l_m of the Jacobian $f'(u_{i+\frac{1}{2}})$ are needed for the local characteristic decomposition. The WENO procedure is used on

$$v_j^\pm = R^{-1} f_j^\pm, \quad j \text{ in a neighborhood of } i, \tag{2.4}$$

where $R = (r_1, \dots, r_n)$ is the matrix whose columns are the right eigenvectors of $f'(u_{i+\frac{1}{2}})$. The numerical fluxes $\hat{v}_{i+\frac{1}{2}}^\pm$ thus computed are then projected back into the physical space by left multiplying with R , yielding finally the numerical fluxes in the physical space.

With the numerical fluxes $\hat{f}_{i+\frac{1}{2}}$, $f(u)_x$ is approximated by (2.1) to high order accuracy at $x = x_i$. Together with a TVD high order Runge–Kutta time discretization [18], this completes a high order WENO scheme. Multidimensional problems are handled in the same fashion, with each derivative approximated along the line of the relevant variable. Again, we refer to [9,17] for further details.

3. A balance of the flux and the source term

In this section we design a finite difference high order WENO-LF scheme for the shallow water equation, with the objective of keeping the exact C-property without reducing the high order accuracy of the scheme. The scheme reduces to the original WENO-LF scheme described in the previous section when the bottom is flat ($b_x = 0$). We start with the description in the one dimensional case. First, we split the source term into two separate terms in the discretization and prove, if written in this form, any linear scheme can maintain the exact C-property. Next, we apply the nonlinear WENO procedure with a small modification and prove that it can also maintain the exact C-property without losing high order accuracy.

We now describe the details. For the shallow water equation (1.1), we split the source term $-ghb_x$ into two terms $(\frac{1}{2}gb^2)_x - g(h+b)b_x$. Hence the equations become

$$\begin{aligned} h_t + (hu)_x &= 0, \\ (hu)_t + \left(hu^2 + \frac{1}{2}gh^2\right)_x &= \left(\frac{1}{2}gb^2\right)_x - g(h+b)b_x, \end{aligned} \quad (3.1)$$

which will be denoted by

$$U_t + f(U)_x = G_1 + G_2, \quad (3.2)$$

where $U = (h, hu)^T$ with the superscript ‘T’ denoting the transpose, $f(U)$ is the flux term and G_1, G_2 are the two source terms.

As we will see below, the special splitting of the source term in (3.1) is crucial for the design of our high order schemes satisfying the exact C-property. It should be noted that the two derivative terms on the right-hand side of (3.1) involve only known functions, not the solution h and u . It is important *not* to include any derivatives of the unknown solution h and u on the right-hand side source term. Otherwise, conservation and convergence towards weak solutions will be problematic for discontinuous solutions.

As usual, we define a linear finite difference operator D to be one satisfying $D(af_1 + bf_2) = aD(f_1) + bD(f_2)$ for constants a, b and arbitrary grid functions f_1 and f_2 . A scheme for (3.1) is said to be a linear scheme if all the spatial derivatives are approximated by linear finite difference operators. For the still water stationary solution of (3.1), we have

$$h + b = \text{constant} \quad \text{and} \quad hu = 0. \quad (3.3)$$

For any consistent linear scheme, the first equation $(hu)_x = 0$ is satisfied exactly since $hu = 0$. The second equation has the truncation error

$$D_1\left(hu^2 + \frac{1}{2}gh^2\right) - D_2\left(\frac{1}{2}gb^2\right) + g(h+b)D_3(b),$$

where D_1, D_2 and D_3 are linear finite difference operators. Since $hu = 0$, this truncation error reduces to

$$D_1\left(\frac{1}{2}gh^2\right) - D_2\left(\frac{1}{2}gb^2\right) + g(h+b)D_3(b).$$

We further restrict our attention to linear schemes which satisfy

$$D_1 = D_2 = D_3 = D \quad (3.4)$$

for the still water stationary solutions. For such linear schemes we have

Proposition 3.1. *Linear schemes for the shallow water equation (3.1) satisfying (3.4) for the still water stationary solutions (3.3) can maintain the exact C-property.*

Proof. For still water stationary solutions (3.3), linear schemes satisfying (3.4) is exact for the first equation $(hu)_x = 0$, and the truncation error for the second equation reduces to

$$D\left(\frac{1}{2}gh^2\right) - D\left(\frac{1}{2}gb^2\right) + g(h+b)D(b) = D\left(\frac{1}{2}gh^2 - \frac{1}{2}gb^2 + g(h+b)b\right) = D\left(\frac{1}{2}g(h+b)^2\right) = 0,$$

where the first equality is due to the linearity of D and the fact that $h+b = \text{constant}$; the second equality is just a simple regrouping of terms inside the parenthesis, and the last equality is due to the fact that $h+b = \text{constant}$ and the consistency of the finite difference operator D . This finishes the proof. \square

Of course, the high order finite difference WENO schemes described in the previous section are nonlinear. The nonlinearity comes from the nonlinear weights, which in turn comes from the nonlinearity of the smooth indicators β_r measuring the smoothness of the functions f^+ and f^- . We would like to make minor modifications to these high order finite difference WENO schemes, so that the exact C-property is maintained and accuracy and nonlinear stability are not affected.

To present the basic ideas, we first consider the situation when the WENO scheme is used without the flux splitting and the local characteristic decomposition. In this case the smoothness indicators β_r measure the smoothness of each component of the flux function $f(U)$. The first equation in (3.1) does not cause a problem for the still water solution, as $hu = 0$ and the consistent WENO approximation to $(hu)_x$ is exact. For the second equation in (3.1), there are three derivative terms, $(hu^2 + \frac{1}{2}gh^2)_x$, $(\frac{1}{2}gb^2)_x$ and b_x , that must be approximated. The approximation to the flux derivative term $(hu^2 + \frac{1}{2}gh^2)_x$ proceeds as before using the WENO approximation. We notice that the WENO approximation to d'_x where $d = hu^2 + \frac{1}{2}gh^2$ can be eventually written out as

$$d_x|_{x=x_i} \approx \sum_{k=-r}^r a_k d_{i+k} \equiv D_d(d)_i, \tag{3.5}$$

where $r = 3$ for the fifth order WENO approximation and the coefficients a_k depend nonlinearly on the smoothness indicators involving the grid function d . The key idea now is to use the difference operator D_d with $d = hu^2 + \frac{1}{2}gh^2$ fixed, namely to use the same coefficients a_k obtained through the smoothness indicators of $d = hu^2 + \frac{1}{2}gh^2$, and apply this difference operator D_d to approximate $(\frac{1}{2}gb^2)_x$ and b_x in the source terms. Thus

$$\left(\frac{1}{2}gb^2\right)_x \Big|_{x=x_i} \approx \sum_{k=-r}^r a_k \left(\frac{1}{2}gb^2\right)_{i+k} \equiv D_d\left(\frac{1}{2}gb^2\right)_i,$$

$$b_x|_{x=x_i} \approx \sum_{k=-r}^r a_k b_{i+k} \equiv D_d(b)_i.$$

Clearly, the finite difference operator D_d , obtained from the fifth order WENO procedure, is a fifth order accurate approximation to the first derivative on any grid function, thus our approximation to the source terms is also fifth order accurate. The approximation of $(\frac{1}{2}gb^2)_x$ can even be absorbed together with the approximation of the flux derivative term $(hu^2 + \frac{1}{2}gh^2)_x$ in actual implementation to save cost (of course, the smoothness indicators to determine the nonlinear weights in the approximation would still be based on $hu^2 + \frac{1}{2}gh^2$). A key observation is that the finite difference operator D_d , with the coefficients a_k based on the smoothness indicators of $d = hu^2 + \frac{1}{2}gh^2$ fixed, is a linear operator on any grid functions, i.e.,

$$D_d(af_1 + bf_2) = aD_d(f_1) + bD_d(f_2)$$

for constants a, b and arbitrary grid functions f_1 and f_2 . Thus the proof of Proposition 3.1 will go through and we can prove that the component-wise WENO scheme, without the flux splitting or local characteristic decomposition, and with the special handling of the source terms described above, maintains exactly the C-property.

Next, we look at the situation when the local characteristic decomposition is invoked in the WENO procedure. When computing the numerical flux at $x_{i+\frac{1}{2}}$, the local characteristic matrix R , consisting of the right eigenvectors of the Jacobian at $u_{i+\frac{1}{2}}$, is fixed, and neighboring point values of the grid functions needed for computing the numerical flux is projected to the local characteristic fields determined by R^{-1} . Therefore, (3.5) still holds, with $d = (hu, hu^2 + \frac{1}{2}gh^2)^T$ now being a vector grid function and a_k are 2×2 matrices depending nonlinearly on the smoothness indicators involving the grid function d . The key idea is still to use the difference operator D_d with $d = (hu, hu^2 + \frac{1}{2}gh^2)^T$ fixed, and apply it to approximate $(0, \frac{1}{2}gb^2)_x^T$

and $(0, b)_x^T$ in the source terms. In actual implementation, we can still absorb the approximation of $(0, \frac{1}{2}gb^2)_x^T$ into that of the flux derivative term $(hu, hu^2 + \frac{1}{2}gh^2)_x^T$ to save computational cost. The remaining arguments stay the same as above, and we can prove that the WENO scheme with a local characteristic decomposition, but without the flux splitting, and with the special handling of the source terms described above, maintains exactly the C-property.

Finally, we consider WENO schemes with a Lax–Friedrichs flux splitting, such as the WENO-LF and WENO-LLF schemes. Now the flux $f(U)$ is written as a sum of $f^+(U)$ and $f^-(U)$, defined by

$$f^\pm(U) = \frac{1}{2} \left[\begin{pmatrix} hu \\ hu^2 + \frac{1}{2}gh^2 \end{pmatrix} \pm \alpha_i \begin{pmatrix} h \\ hu \end{pmatrix} \right] \tag{3.6}$$

for the i th characteristic field, where $\alpha_i = \max_u |\lambda_i(u)|$ with $\lambda_i(u)$ being the i th eigenvalue of the Jacobian $f'(U)$, see [9,17] for more details. We now make a modification to this flux splitting, by replacing $\pm \alpha_i \begin{pmatrix} h \\ hu \end{pmatrix}$ in (3.6) with $\pm \alpha_i \begin{pmatrix} h+b \\ hu \end{pmatrix}$. The flux splitting (3.6) now becomes

$$f^\pm(U) = \frac{1}{2} \left[\begin{pmatrix} hu \\ hu^2 + \frac{1}{2}gh^2 \end{pmatrix} \pm \alpha_i \begin{pmatrix} h+b \\ hu \end{pmatrix} \right]. \tag{3.7}$$

This modification is justified since b does not depend on the time t , hence the first equation in (1.1) can also be considered as an evolution equation for $h+b$ instead of for h . Similar techniques are used in the surface gradient method by Zhou et al. [24]. Our motivation for using $\pm \alpha_i \begin{pmatrix} h+b \\ hu \end{pmatrix}$ instead of the original $\pm \alpha_i \begin{pmatrix} h \\ hu \end{pmatrix}$ in the flux splitting, is that the former becomes a constant vector for the still water stationary solution (3.3). Thus for this still water stationary solution, by the consistency of the WENO approximation, the effect of this viscosity term $\pm \alpha_i \begin{pmatrix} h+b \\ hu \end{pmatrix}$ towards the approximation of $f(U)_x$ is zero. Clearly, (3.5) can represent the flux splitting WENO approximation, with a simple splitting $f^\pm(U) = \frac{1}{2}f(U)$, with $d = (hu, hu^2 + \frac{1}{2}gh^2)^T$ being a vector grid function and a_k being 2×2 matrices depending nonlinearly on the smoothness indicators involving the grid function $f^\pm(U)$ in (3.7). What we have shown above is that, for the still water stationary solution, this is also the flux splitting WENO approximation with the modified Lax-Friedrich flux splitting (3.7). As before, the key idea now is to use the difference operator D_d in (3.5) with smoothness indicators, hence the nonlinear weights obtained from $f^\pm(U)$ in (3.7) fixed, and apply it to approximate $(0, \frac{1}{2}gb^2)_x^T$ and $(0, b)_x^T$ in the source terms. This amounts to split also the two derivatives in the source terms as

$$\begin{pmatrix} 0 \\ \frac{1}{2}gb^2 \end{pmatrix}_x = \frac{1}{2} \begin{pmatrix} 0 \\ \frac{1}{2}gb^2 \end{pmatrix}_x + \frac{1}{2} \begin{pmatrix} 0 \\ \frac{1}{2}gb^2 \end{pmatrix}_x, \quad \begin{pmatrix} 0 \\ b \end{pmatrix}_x = \frac{1}{2} \begin{pmatrix} 0 \\ b \end{pmatrix}_x + \frac{1}{2} \begin{pmatrix} 0 \\ b \end{pmatrix}_x, \tag{3.8}$$

and apply the same flux split WENO procedure to approximate them, namely, one half of each source term is approximated by the difference operator with coefficients a_k obtained from the computation of f^+ , and the remaining part by the difference operator with coefficients a_k obtained from the computation of f^- . In actual implementation, we can still absorb the approximation of $(0, \frac{1}{2}gb^2)_x^T$ into that of the flux derivative term $(hu, hu^2 + \frac{1}{2}gh^2)_x^T$ to save computational cost. The remaining arguments stay the same as above, and we can prove that the WENO scheme with a local characteristic decomposition and a flux splitting (3.7), and with the special handling of the source terms described above, maintains exactly the C-property.

We now summarize the complete procedure of the high order finite difference WENO-LF or WENO-LLF scheme with a local characteristic decomposition and a flux splitting, for solving the shallow water equation (1.1):

1. Split the source term and write the equation in the form (3.1).
2. Perform the usual WENO-LF or WENO-LLF approximation on the flux derivative $\left(hu^2 + \frac{1}{2}gh^2 \right)_x$, with a modified flux splitting (3.7) and using the local characteristic decomposition.
3. Split the two derivative terms in the source terms on the right-hand side of (3.1) as in (3.8), and perform the same WENO approximation which is used in step 2 above, using the local characteristic decomposition and the same nonlinear weights, to approximate these two derivative terms. In actual implementation, the approximation of the first derivative term $\left(\begin{matrix} 0 \\ \frac{1}{2}gb^2 \end{matrix} \right)_x$ can be absorbed into the approximation of the flux derivative $\left(hu^2 + \frac{1}{2}gh^2 \right)_x$, to save computational cost.
4. Add up the residues and forward in time.

With this computational procedure, we have already shown above the exact C-property and high order accuracy.

Proposition 3.2. *The WENO-LF or WENO-LLF schemes as stated above can maintain the exact C-property and their original high order accuracy.*

Even though we have described the algorithm using the WENO-LF and WENO-LLF flux splitting form, the algorithm can clearly also be defined with the same properties for other finite difference WENO schemes in [9,17], such as WENO-Roe and WENO-Roe with an entropy fix.

4. One dimensional numerical results

In this section we present numerical results of our fifth order finite difference WENO-LF scheme satisfying the exact C-property for the one dimensional shallow water equation (1.1). In all the examples, time discretization is by the classical fourth order Runge–Kutta method, and the CFL number is taken as 0.6, except for the accuracy tests where smaller time step is taken to ensure that spatial errors dominate. The gravitation constant g is taken as 9.812 m/s².

4.1. Test for the exact C-property

The purpose of the first test problem is to verify that the scheme indeed maintains the exact C-property over a nonflat bottom. We choose two different functions for the bottom topography given by $(0 \leq x \leq 10)$:

$$b(x) = 5e^{-\frac{2}{3}(x-5)^2}, \tag{4.1}$$

which is smooth, and

$$b(x) = \begin{cases} 4 & \text{if } 4 \leq x \leq 8, \\ 0 & \text{otherwise,} \end{cases} \tag{4.2}$$

which is discontinuous. The initial data is the stationary solution:

$$h + b = 10, \quad hu = 0.$$

This steady state should be exactly preserved. We compute the solution until $t = 0.5$ using $N = 200$ uniform mesh points. The computed surface level $h + b$ and the bottom b for (4.1) are plotted in Fig. 1. In order to demonstrate that the exact C-property is indeed maintained up to round-off error, we use single precision, double precision and quadruple precision to perform the computation, and show the L^1 and L^∞ errors for the water height h (note: h in this case is not a constant function!) and the discharge hu in Tables 1 and 2 for

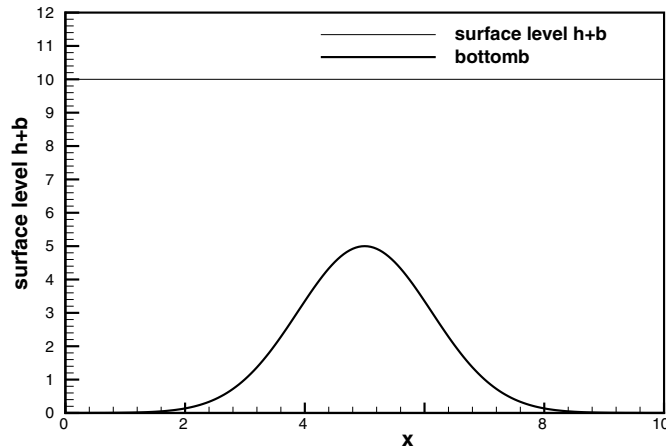


Fig. 1. The surface level $h + b$ and the bottom b for the stationary flow over a smooth bump.

Table 1

L^1 and L^∞ errors for different precisions for the stationary solution with a smooth bottom (4.1)

Precision	L^1 error		L^∞ error	
	h	hu	h	hu
Single	3.13E-07	1.05E-05	9.54E-07	4.85E-05
Double	1.24E-15	2.34E-14	7.11E-15	8.65E-14
Quadruple	1.62E-33	2.11E-32	6.16E-33	8.74E-32

Table 2

L^1 and L^∞ errors for different precisions for the stationary solution with a nonsmooth bottom (4.2)

Precision	L^1 error		L^∞ error	
	h	hu	h	hu
Single	2.28E-07	3.61E-06	1.91E-06	2.37E-05
Double	1.14E-15	9.05E-15	3.55E-15	4.46E-14
Quadruple	1.30E-33	1.40E-32	4.62E-33	5.64E-32

the two bottom functions (4.1) and (4.2) and different precisions. We can clearly see that the L^1 and L^∞ errors are at the level of round-off errors for different precisions, verifying the exact C-property.

We have also computed stationary solutions using initial conditions which are not the steady state solutions and letting time evolve into a steady state, obtaining similar results with the exact C-property.

4.2. Testing the orders of accuracy

In this example we will test the fifth order accuracy of our scheme for a smooth solution. There are some known exact solutions (in closed form) to the shallow water equation with nonflat bottom in the literature, e.g. [21], but these solutions have special properties, making the leading terms in the truncation errors of

Table 3
 L^1 errors and numerical orders of accuracy for the example in Section 4.3

No. of points	CFL	Balanced WENO				Original WENO			
		h		hu		h		hu	
		L^1 error	Order	L^1 error	Order	L^1 error	Order	L^1 error	Order
25	0.6	1.70E–02		1.06E–01		1.96E–02		1.02E–01	
50	0.6	2.17E–03	2.97	1.95E–02	2.45	2.46E–03	2.99	1.82E–02	2.49
100	0.6	3.33E–04	2.71	2.83E–03	2.78	3.19E–04	2.95	2.79E–03	2.70
200	0.6	2.36E–05	3.82	2.04E–04	3.80	2.50E–05	3.67	2.18E–04	3.68
400	0.6	9.67E–07	4.61	8.38E–06	4.61	1.03E–06	4.59	9.07E–06	4.59
800	0.6	3.38E–08	4.84	2.94E–07	4.83	3.61E–08	4.84	3.15E–07	4.85
1600	0.4	1.08E–09	4.97	9.34E–09	4.97	1.15E–09	4.97	1.00E–08	4.98

“Balanced WENO” refers to the WENO scheme with exact C-property and “original WENO” refers to the WENO scheme with the source terms directly added as point values at the grids.

many schemes vanish, hence they are not generic test cases for accuracy. We have therefore chosen to use the following bottom function and initial conditions:

$$b(x) = \sin^2(\pi x), \quad h(x, 0) = 5 + e^{\cos(2\pi x)}, \quad (hu)(x, 0) = \sin(\cos(2\pi x)), \quad x \in [0, 1]$$

with periodic boundary conditions. Since the exact solution is not known explicitly for this case, we use the same fifth order WENO scheme with $N = 25,600$ points to compute a reference solution, and treat this reference solution as the exact solution in computing the numerical errors. We compute up to $t = 0.1$ when the solution is still smooth (shocks develop later in time for this problem). Table 3 contains the L^1 errors and numerical orders of accuracy. We can clearly see that fifth order accuracy is achieved for this example. For comparison, we also list the L^1 errors and numerical orders of accuracy when the original fifth order WENO scheme [9] with the source term directly added to the residue as a point value at the grid x_i (hence not a C-property satisfying scheme) is used on the same problem. We can clearly see that the errors of the two schemes are comparable. For this problem, the solution is far from a still water stationary solution, hence our exact C-property satisfying WENO scheme is not expected to have an advantage in accuracy. Table 3 shows that it does not have a disadvantage either comparing with the traditional WENO scheme using point value treatment of source terms.

4.3. A small perturbation of a steady-state water

The following quasi-stationary test case was proposed by LeVeque [12]. It was chosen to demonstrate the capability of the proposed scheme for computations on a rapidly varying flow over a smooth bed, and the perturbation of a stationary state.

The bottom topography consists of one hump:

$$b(x) = \begin{cases} 0.25(\cos(10\pi(x - 1.5)) + 1) & \text{if } 1.4 \leq x \leq 1.6, \\ 0 & \text{otherwise.} \end{cases} \tag{4.3}$$

The initial conditions are given with

$$(hu)(x, 0) = 0 \quad \text{and} \quad h(x, 0) = \begin{cases} 1 - b(x) + \epsilon & \text{if } 1.1 \leq x \leq 1.2, \\ 1 - b(x) & \text{otherwise,} \end{cases} \tag{4.4}$$

where ϵ is a nonzero perturbation constant. Two cases have been run: $\epsilon = 0.2$ (big pulse) and $\epsilon = 0.001$ (small pulse). Theoretically, for small ϵ , this disturbance should split into two waves, propagating left

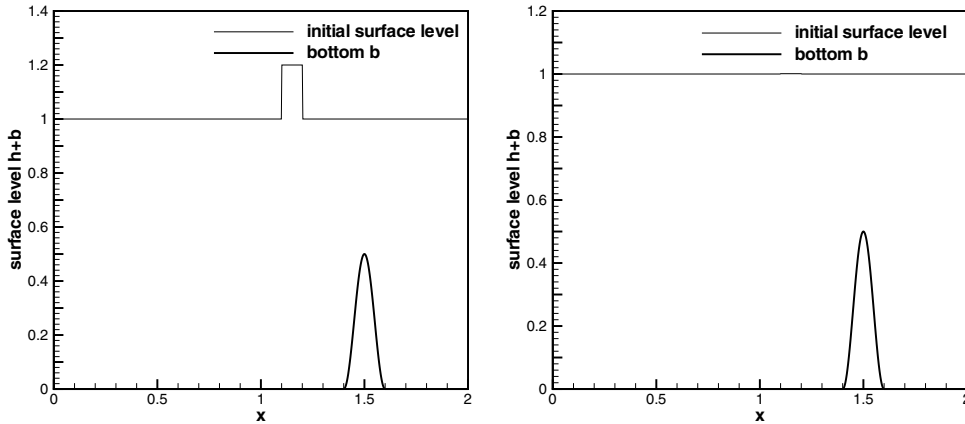


Fig. 2. The initial surface level $h + b$ and the bottom b for a small perturbation of a steady-state water. Left: a big pulse $\epsilon = 0.2$; right: a small pulse $\epsilon = 0.001$.

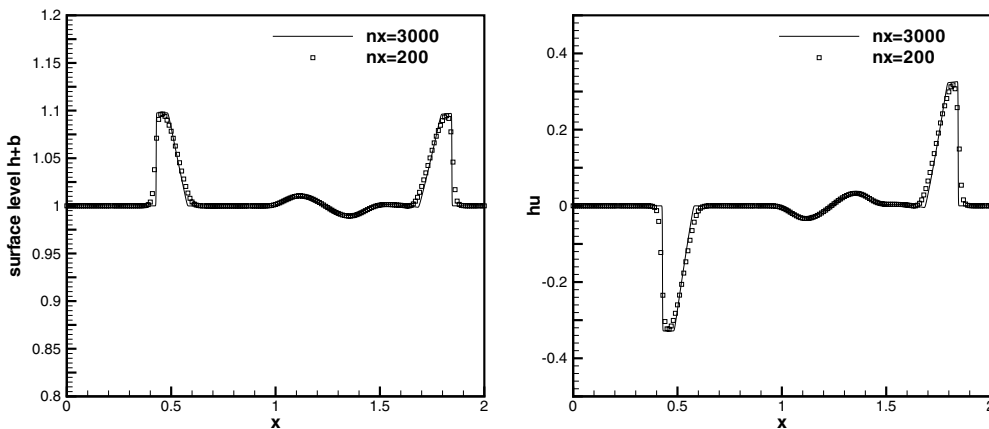


Fig. 3. Small perturbation of a steady-state water with a big pulse. $t = 0.2$ s. Left: surface level $h + b$; right: the discharge hu .

and right at the characteristic speeds $\pm\sqrt{gh}$. Many numerical methods have difficulty with the calculations involving such small perturbations of the water surface [12]. Both sets of initial conditions are shown in Fig. 2. The solution at time $t = 0.2$ s for the big pulse $\epsilon = 0.2$, obtained on a 200 cell uniform grid with simple transmissive boundary conditions, and compared with a 3000 cell solution, is shown in Fig. 3. The one for the small pulse $\epsilon = 0.001$ is shown in Fig. 4. For this small pulse problem, we take $\epsilon = 10^{-9}$ in the WENO weight formula (2.2), such that it is smaller than the square of the perturbation. At this time, the downstream-traveling water pulse has already passed the bump. In the figures, we can clearly see that there are no spurious numerical oscillations, verifying the essentially nonoscillatory property of the modified WENO-LF scheme.

4.4. The dam breaking problem over a rectangular bump

In this example we simulate the dam breaking problem over a rectangular bump, which involves a rapidly varying flow over a discontinuous bottom topography. This example was used in [21].

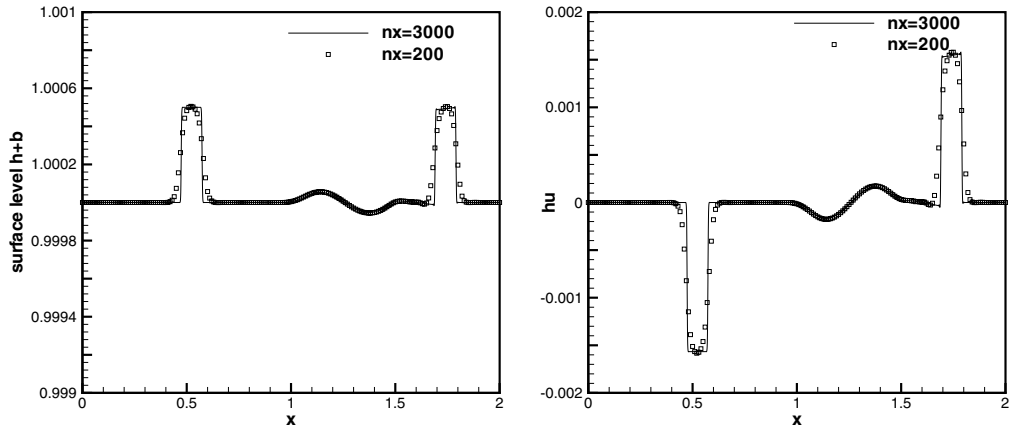


Fig. 4. Small perturbation of a steady-state water with a small pulse. $t = 0.2$ s. Left: surface level $h + b$; right: the discharge hu .

The bottom topography takes the form:

$$b(x) = \begin{cases} 8 & \text{if } |x - 750| \leq 1500/8, \\ 0 & \text{otherwise} \end{cases} \quad (4.5)$$

for $x \in [0, 1500]$. The initial conditions are

$$(hu)(x, 0) = 0 \quad \text{and} \quad h(x, 0) = \begin{cases} 20 - b(x) & \text{if } x \leq 750, \\ 15 - b(x) & \text{otherwise.} \end{cases} \quad (4.6)$$

The numerical results with 500 uniform points (and a comparison with the results using 5000 uniform points) are shown in Figs. 5 and 6, with two different ending time $t = 15$ s and $t = 60$ s. In this example, the water height $h(x)$ is discontinuous at the points $x = 562.5$ and $x = 937.5$, while the surface level $h(x) + b(x)$ is smooth there. Our scheme works well for this example, giving well resolved, nonoscillatory solutions using 500 points which agree with the converged results using 5000 points.

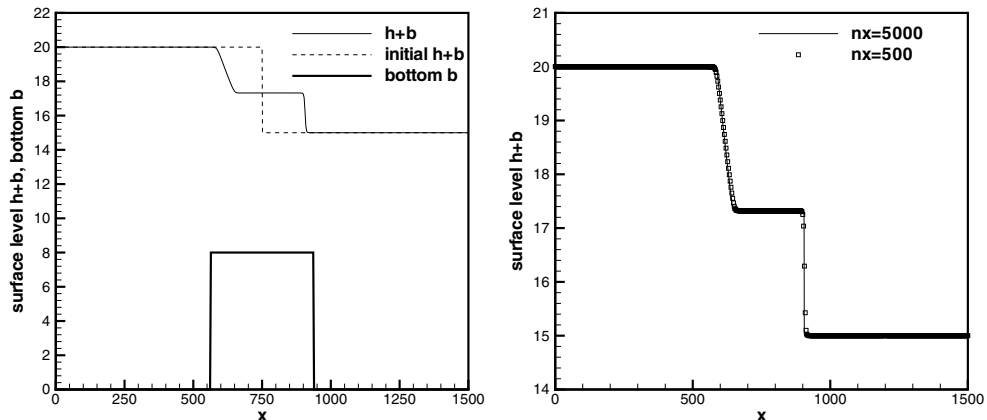


Fig. 5. The surface level $h + b$ for the dam breaking problem at time $t = 15$ s. Left: the numerical solution using 500 grid points, plotted with the initial condition and the bottom topography; Right: the numerical solution using 500 and 5000 grid points.

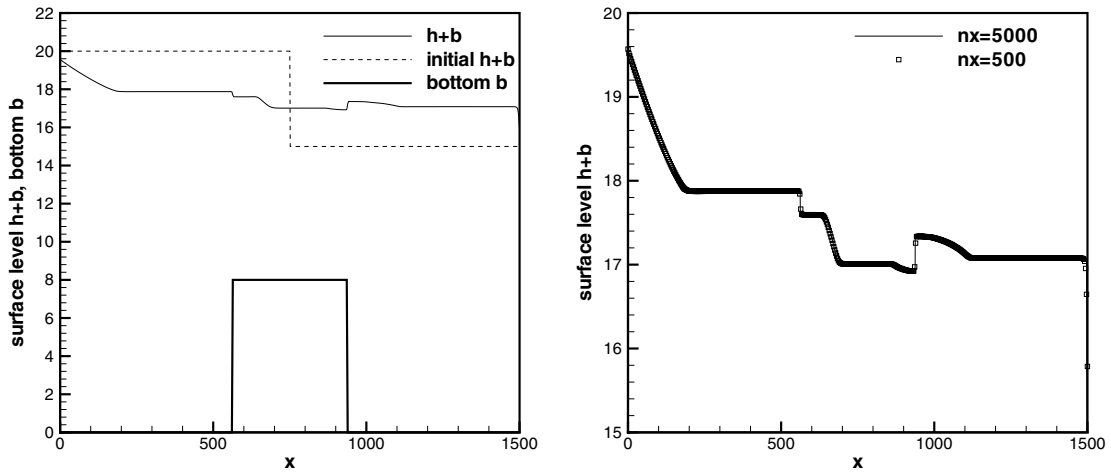


Fig. 6. The surface level $h + b$ for the dam breaking problem at time $t = 60$ s. Left: the numerical solution using 500 grid points, plotted with the initial condition and the bottom topography; Right: the numerical solution using 500 and 5000 grid points.

4.5. Steady flow over a hump

The purpose of this test case is to study the convergence in time towards steady flow over a bump. These are classical test problems for transcritical and subcritical flows, and they are widely used to test numerical schemes for shallow water equations. For example, they have been considered by the *working group on dam break modeling* [5], and have been used as a test case in, e.g., [20].

The bottom function is given by

$$b(x) = \begin{cases} 0.2 - 0.05(x - 10)^2 & \text{if } 8 \leq x \leq 12, \\ 0 & \text{otherwise} \end{cases} \quad (4.7)$$

for a channel of length 25 m. The initial conditions are taken as

$$h(x, 0) = 0.5 - b(x) \quad \text{and} \quad u(x, 0) = 0.$$

Depending on different boundary conditions, the flow can be subcritical or transcritical with or without a steady shock. The computational parameters common for all three cases are: uniform mesh size $\Delta x = 0.125$ m, ending time $t = 200$ s. Analytical solutions for the various cases are given in [5].

(a) Transcritical flow without a shock.

- upstream: The discharge $hu = 1.53 \text{ m}^3/\text{s}$ is imposed.
- downstream: The water height $h = 0.66$ m is imposed when the flow is subcritical.

The surface level $h + b$ and the discharge hu , as the numerical flux for the water height h in Eq. (1.1), are plotted in Fig. 7, which show very good agreement with the analytical solution. The correct capturing of the discharge hu is usually more difficult than the surface level $h + b$, as noticed by many authors. In Fig. 8, we compare the pointwise errors of the numerical solutions obtained with 200 and 400 uniform grid points. The convergence history, measured by the L^1 norm of the residue, is given in Fig. 9, left.

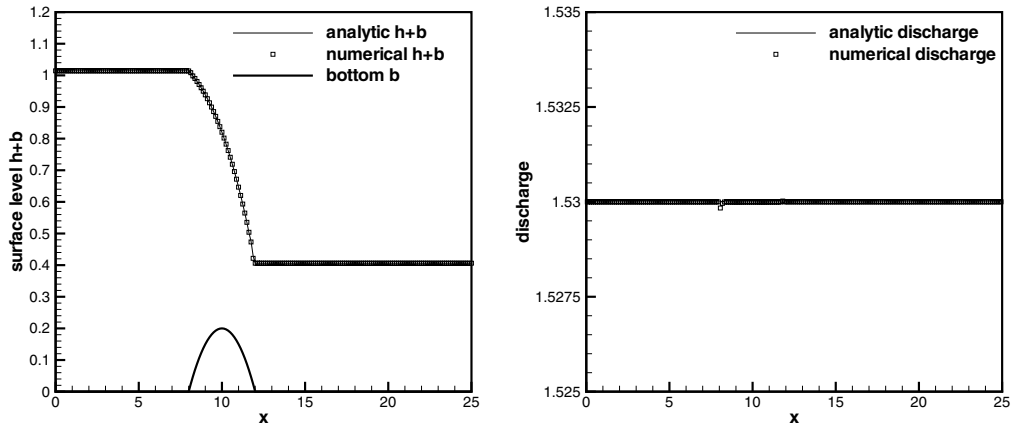


Fig. 7. Steady transcritical flow over a bump without a shock. Left: the surface level $h + b$; right: the discharge hu as the numerical flux for the water height h .

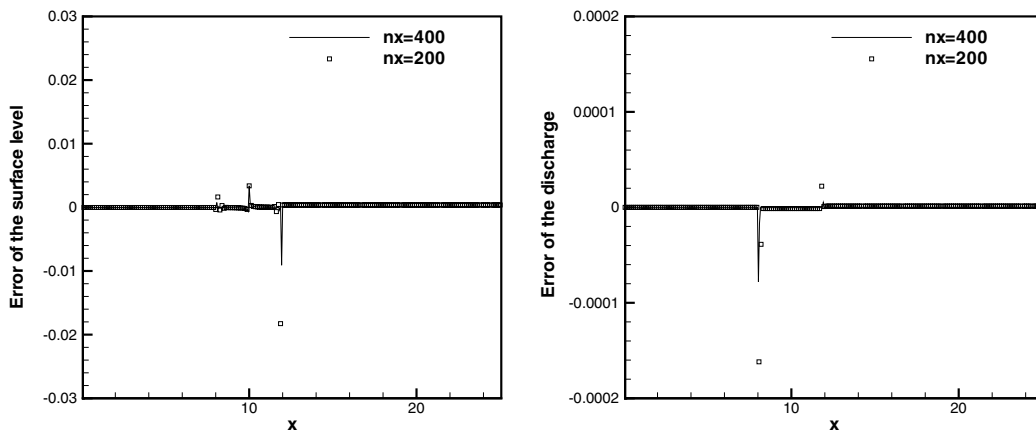


Fig. 8. Steady transcritical flow over a bump without a shock. Pointwise error comparison between numerical solutions using 200 and 400 grid points. Left: the surface level $h + b$; right: the discharge hu as the numerical flux for the water height h .

(b) Transcritical flow with a shock.

- upstream: The discharge $hu = 0.18 \text{ m}^3/\text{s}$ is imposed.
- downstream: The water height $h = 0.33 \text{ m}$ is imposed.

In this case, the Froude number $Fr = u/\sqrt{gh}$ increases to a value larger than one above the bump, and then decreases to less than one. A stationary shock can appear on the surface. The surface level $h + b$ and the discharge hu , as the numerical flux for the water height h in Eq. (1.1), are plotted in Fig. 10, which show nonoscillatory results in good agreement with the analytical solution. In Fig. 11, we compare the pointwise errors of the numerical solutions obtained with 200 and 400 uniform grid points. The convergence history, measured by the L^1 norm of the residue, is given in Fig. 9, right.

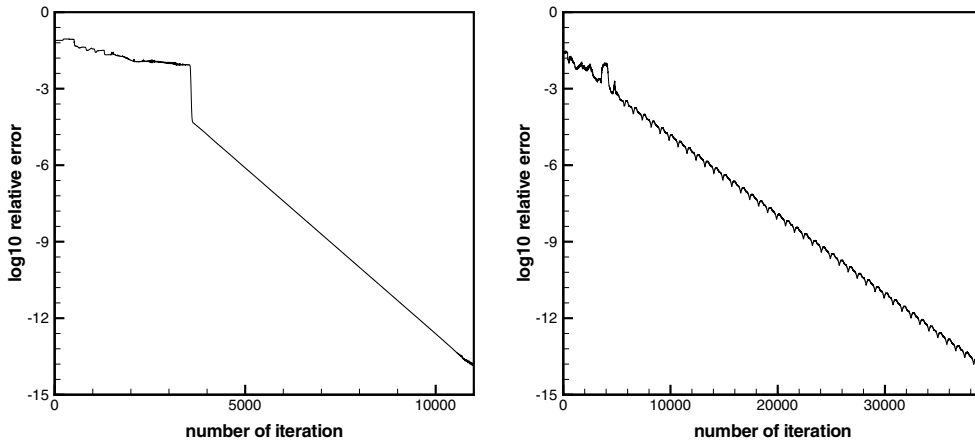


Fig. 9. Convergence history in L^1 residue. Left: steady transcritical flow over a bump without a shock; right: steady transcritical flow over a bump with a shock.

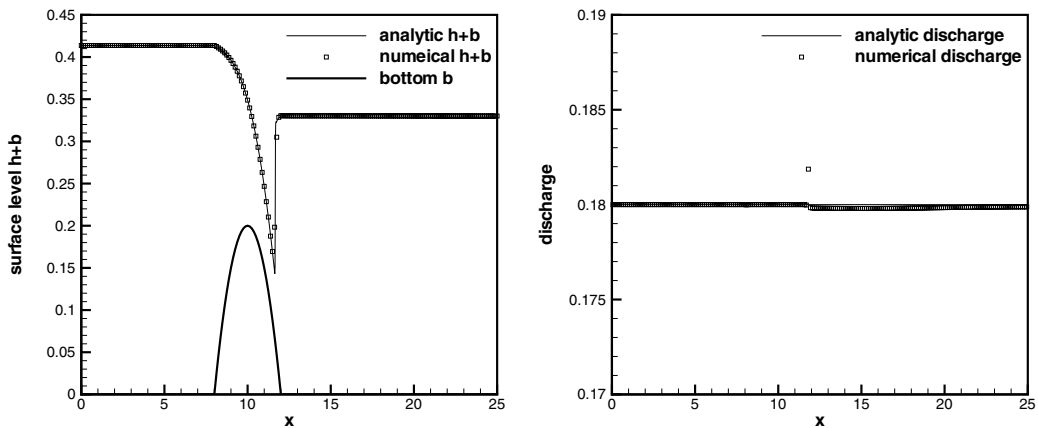


Fig. 10. Steady transcritical flow over a bump with a shock. Left: the surface level $h + b$; right: the discharge hu as the numerical flux for the water height h .

(c) Subcritical flow.

- upstream: The discharge $hu = 4.42 \text{ m}^3/\text{s}$ is imposed.
- downstream: The water height $h = 2 \text{ m}$ is imposed.

This is a subcritical flow. The surface level $h + b$ and the discharge hu , as the numerical flux for the water height h in Eq. (1.1), are plotted in Fig. 12, which are in good agreement with the analytical solution. In Fig. 13, we compare the pointwise errors of the numerical solutions obtained with 200 and 400 uniform grid points.

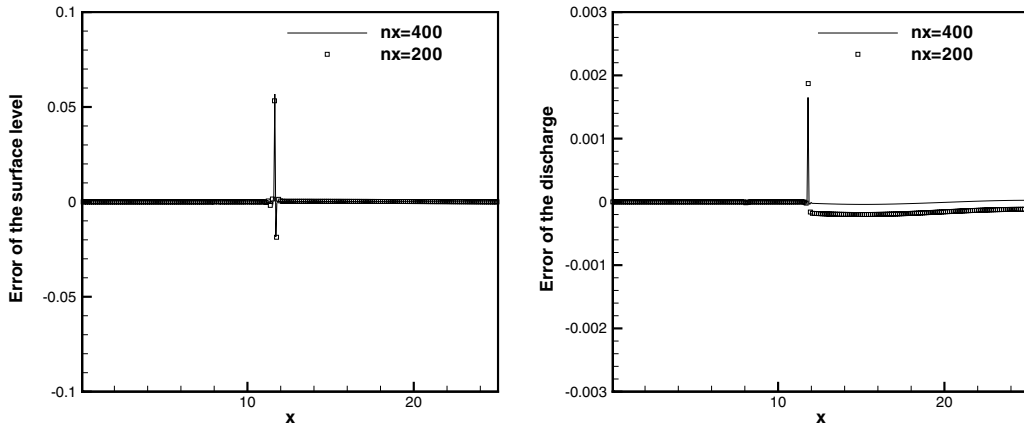


Fig. 11. Steady transcritical flow over a bump with a shock. Pointwise error comparison between numerical solutions using 200 and 400 grid points. Left: the surface level $h + b$; right: the discharge hu as the numerical flux for the water height h .

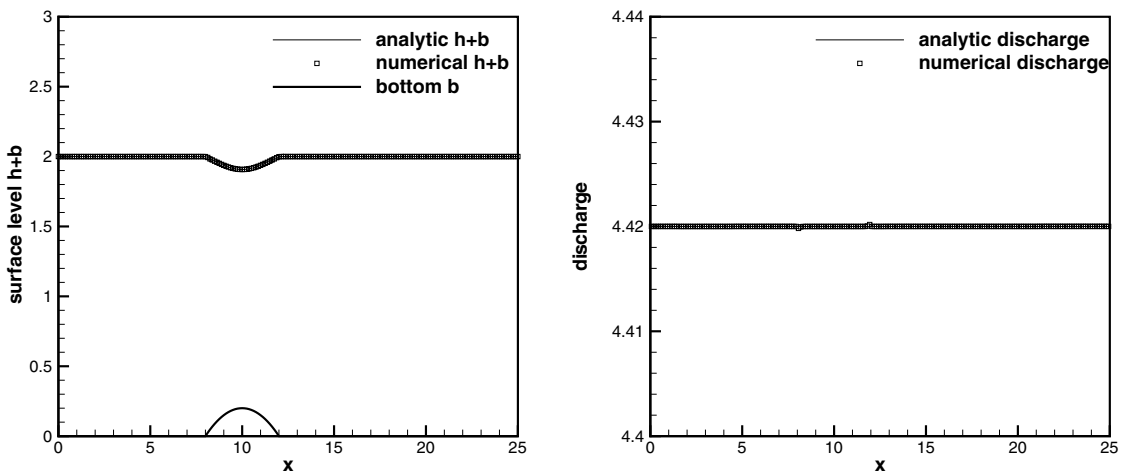


Fig. 12. Steady subcritical flow over a bump. Left: the surface level $h + b$; right: the discharge hu as the numerical flux for the water height h .

4.6. The tidal wave flow

This example was used in [2], in which an almost exact solution (a very good asymptotically derived approximation) was given. We use this example to further test our scheme.

The bottom is defined by

$$b(x) = 10 + \frac{40x}{L} + 10 \sin \left(\pi \left(\frac{4x}{L} - \frac{1}{2} \right) \right),$$

where $L = 14,000$ m is the channel length. If we take the initial and boundary conditions as

$$h(x, 0) = 60.5 - b(x), \quad (hu)(x, 0) = 0,$$

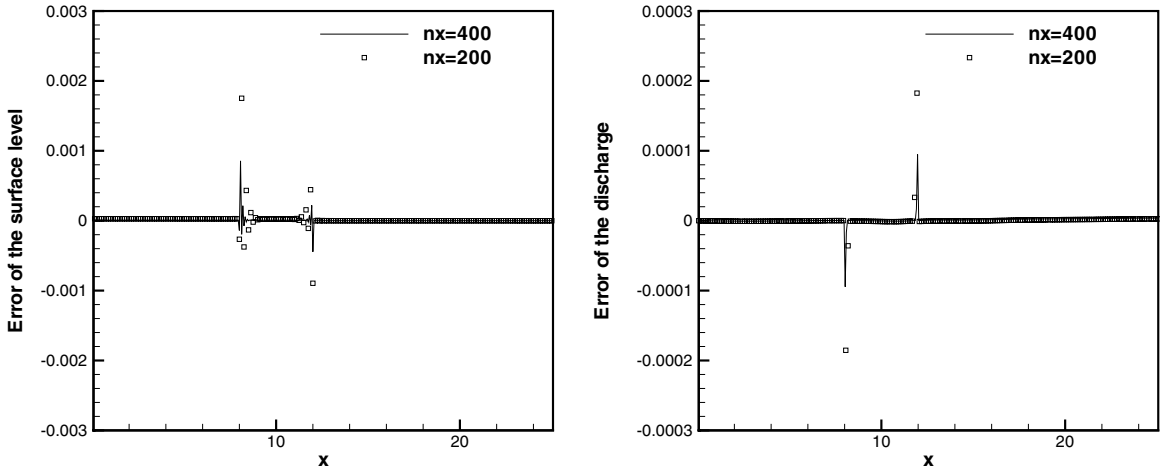


Fig. 13. Steady subcritical flow over a bump. Pointwise error comparison between numerical solutions using 200 and 400 grid points. Left: the surface level $h + b$; right: the discharge hu as the numerical flux for the water height h .

$$h(0, t) = 64.5 - 4 \sin \left(\pi \left(\frac{4t}{86,400} + \frac{1}{2} \right) \right), \quad (hu)(L, t) = 0,$$

a very accurate approximate solution, based on the asymptotic analysis, can be given by [2]

$$h(x, t) = 64.5 - b(x) - 4 \sin \left(\pi \left(\frac{4t}{86,400} + \frac{1}{2} \right) \right)$$

and

$$(hu)(x, t) = \frac{(x - L)\pi}{5400} \cos \left(\pi \left(\frac{4t}{86,400} + \frac{1}{2} \right) \right).$$

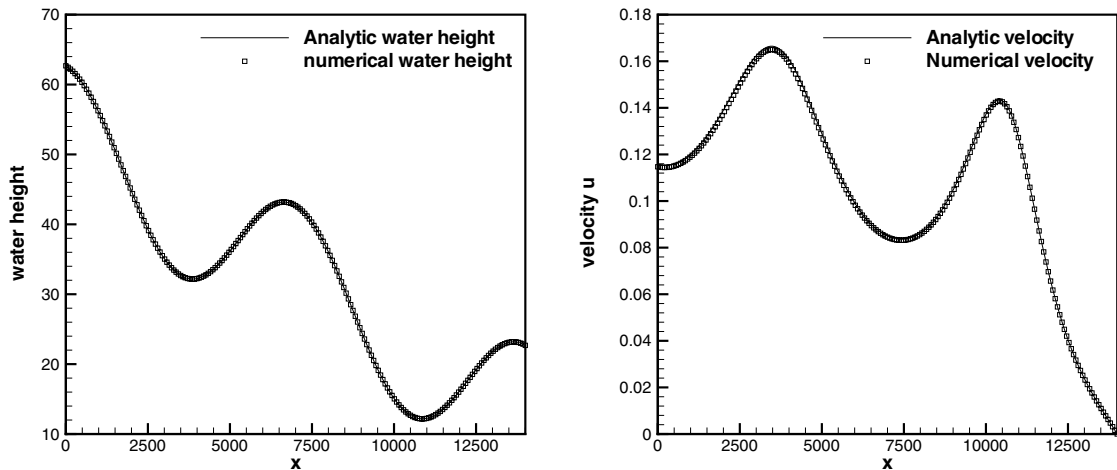


Fig. 14. Numerical and analytic solutions for the tidal wave flow. Left: water height h ; right: velocity u .

We use a uniform mesh size $\Delta x = 70$ m. A comparison of the numerical and analytical results at $t = 7552.13$ s is shown in Fig. 14. Their agreements are very good.

5. Two dimensional shallow water systems

A major advantage of the high order finite difference WENO schemes is that it is straightforward to extend them to multiple space dimensions, by simply approximating each spatial derivative along the relevant coordinate. It turns out that it is also straightforward to extend the high order finite difference WENO schemes with the exact C-property developed in Section 3 to two dimensions. The shallow water system in two space dimensions takes the form:

$$\begin{aligned}
 h_t + (hu)_x + (hv)_y &= 0, \\
 (hu)_t + \left(hu^2 + \frac{1}{2}gh^2\right)_x + (huv)_y &= -ghb_x, \\
 (hv)_t + (huv)_x + \left(hv^2 + \frac{1}{2}gh^2\right)_y &= -ghb_y,
 \end{aligned}
 \tag{5.1}$$

where again h is the water height, (u, v) is the velocity of the fluid, $b(x, y)$ represents the bottom topography and g is the gravitational constant.

Finite difference WENO schemes are very easy to be extended to multidimensional cases. The conservative approximation to the derivative from point values is as simple in multi dimensions as in one dimension. In fact, for fixed j , if we take $w(x) = f(u(x, y_j))$, then we only need to perform the one dimensional WENO approximation to $w(x)$ to obtain an approximation to $w'(x_i) = f_x(u(x_i, y_j))$. See again [9,17] for more details.

The source term is again split as in the one dimensional case

$$-ghb_x = \left(\frac{1}{2}gb^2\right)_x - g(h + b)b_x, \quad -ghb_y = \left(\frac{1}{2}gb^2\right)_y - g(h + b)b_y,$$

and the one dimension procedure described in Section 3 is followed in each of the x and y directions. The residues are then summed up and advancement in time is again by a Runge–Kutta method.

All results proved in the one dimensional case, such as high order accuracy and the exact C-property, are still valid in the two dimensional case.

We now give numerical experiment results for the exact C-property satisfying fifth order WENO-LF scheme in two dimensions. Similar to the one dimensional case, we use the classical fourth order Runge–Kutta time discretization and a CFL number 0.6, except for the accuracy test problem where smaller time step is taken to guarantee that spatial errors dominate.

5.1. Test for the exact C-property in two dimensions

This example is used to check that our scheme indeed maintains the exact C-property over a nonflat bottom. The two dimensional hump

$$b(x, y) = 0.8e^{-50((x-0.5)^2 + (y-0.5)^2)}, \quad x, y \in [0, 1],
 \tag{5.2}$$

is chosen to be the bottom. $h(x, y, 0) = 1 - b(x, y)$ is the initial depth of the water. Initial velocity is set to be zero. This surface should remain flat. The computation is performed to $t = 0.1$ using single, double and quadruple precisions with a 100×100 uniform mesh. Table 4 contains the L^1 errors for the water height h (which is not a constant function) and the discharges hu and hv . We can clearly see that the L^1 errors are at the level of round-off errors for different precisions, verifying the exact C-property.

Table 4
 L^1 errors for different precisions for the stationary solution in Section 5.1

Precision	L^1 error		
	h	hu	hv
Single	2.18E–08	2.32E–07	2.32E–07
Double	7.71E–17	9.36E–16	9.36E–16
Quadruple	7.64E–34	9.33E–34	9.33E–34

5.2. Testing the orders of accuracy

In this example we check the numerical orders of accuracy when the WENO schemes are applied to the following two dimensional problem. The bottom topography and the initial data are given by

$$b(x, y) = \sin(2\pi x) + \cos(2\pi y), \quad h(x, y, 0) = 10 + e^{\sin(2\pi x)} \cos(2\pi y),$$

$$(hu)(x, y, 0) = \sin(\cos(2\pi x)) \sin(2\pi y), \quad (hv)(x, y, 0) = \cos(2\pi x) \cos(\sin(2\pi y))$$

defined over a unit square, with periodic boundary conditions. The terminal time is taken as $t = 0.05$ to avoid the appearance of shocks in the solution. Since the exact solution is not known explicitly for this case, we use the same fifth order WENO scheme with an extremely refined mesh consisting of 1600×1600 grid points to compute a reference solution, and treat this reference solution as the exact solution in computing the numerical errors. Table 5 contains the L^1 errors and orders of accuracy. We can clearly see that fifth order accuracy is achieved in this two dimensional test case.

5.3. A small perturbation of a two dimensional steady-state water

This is a classical example to show the capability of the proposed scheme for the perturbation of the stationary state, given by LeVeque [12]. It is analogous to the test done previously in Section 4.3 in one dimension.

We solve the system in the rectangular domain $[0, 2] \times [0, 1]$. The bottom topography is an isolated elliptical shaped hump:

$$b(x, y) = 0.8e^{-5(x-0.9)^2 - 50(y-0.5)^2}. \quad (5.3)$$

The surface is initially given by

$$h(x, y, 0) = \begin{cases} 1 - b(x, y) + 0.01 & \text{if } 0.05 \leq x \leq 0.15, \\ 1 - b(x, y) & \text{otherwise,} \end{cases} \quad (5.4)$$

$$hu(x, y, 0) = hv(x, y, 0) = 0.$$

Table 5
 L^1 errors and numerical orders of accuracy for the example in Section 5.2

Number of cells	CFL	h		hu		hv	
		L^1 error	Order	L^1 error	Order	L^1 error	Order
25	0.6	1.08E–02		3.23E–02		8.92E–02	
50	0.6	1.30E–03	3.06	2.47E–03	3.70	1.19E–02	2.90
100	0.6	1.06E–04	3.61	1.47E–04	4.07	9.06E–04	3.72
200	0.4	4.82E–06	4.46	6.25E–06	4.56	3.98E–05	4.51
400	0.3	1.79E–07	4.75	2.31E–07	4.76	1.41E–06	4.82
800	0.2	6.30E–09	4.83	8.19E–09	4.82	4.70E–08	4.91

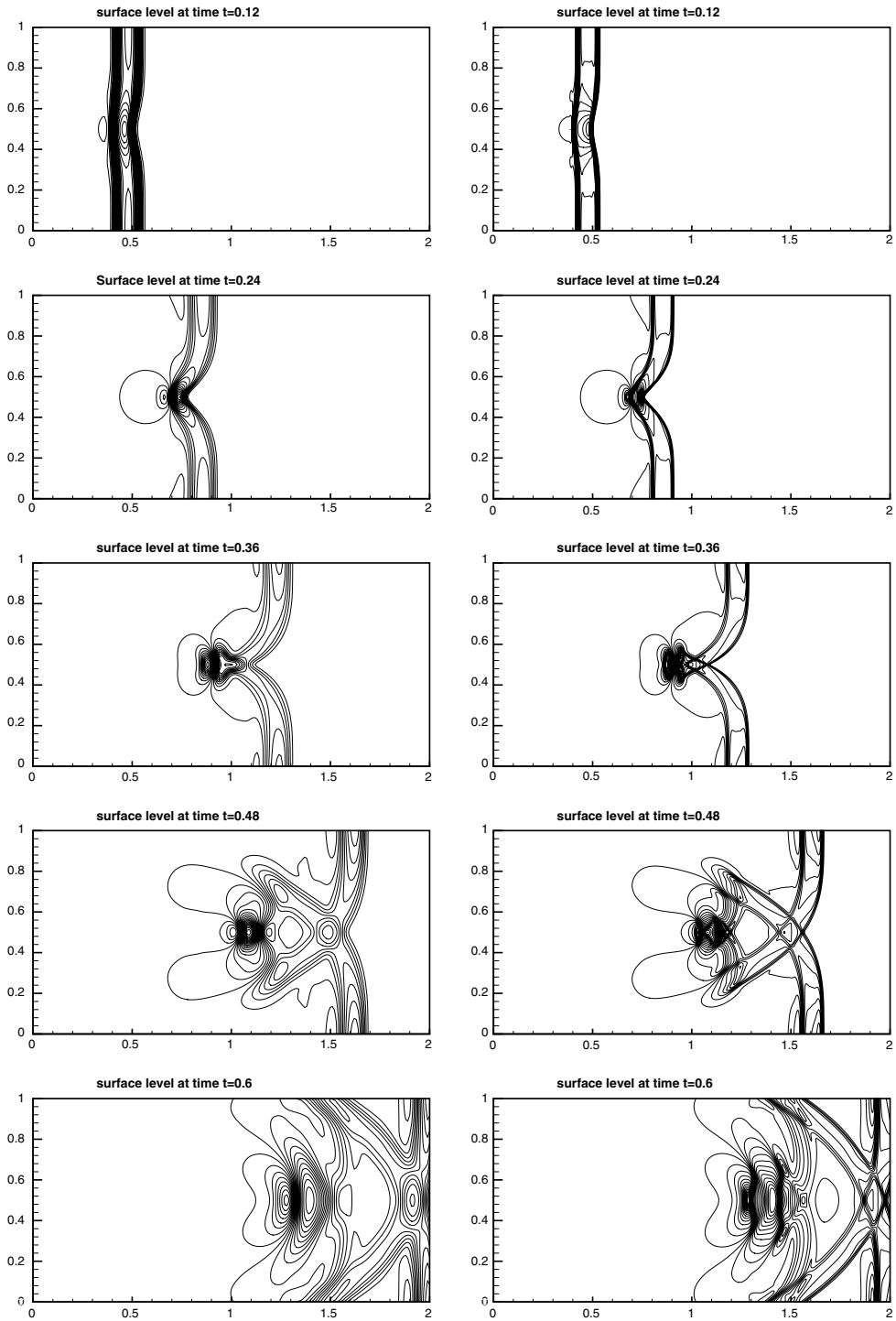


Fig. 15. The contours of the surface level $h + b$ for the problem in Section 5.3. 30 uniformly spaced contour lines. From top to bottom: at time $t = 0.12$ from 0.999703 to 1.00629; at time $t = 0.24$ from 0.994836 to 1.01604; at time $t = 0.36$ from 0.988582 to 1.0117; at time $t = 0.48$ from 0.990344 to 1.00497; and at time $t = 0.6$ from 0.995065 to 1.0056. Left: results with a 200×100 uniform mesh. Right: results with a 600×300 uniform mesh.

So the surface is almost flat except for $0.05 \leq x \leq 0.15$, where h is perturbed upward by 0.01. Fig. 15 displays the right-going disturbance as it propagates past the hump, on two different uniform meshes with 200×100 points and 600×300 points for comparison. The surface level $h + b$ is presented at different time. The results indicate that our scheme can resolve the complex small features of the flow very well.

6. Concluding remarks

In this paper we extend the high order finite difference WENO schemes to solve the shallow water system in one and two space dimensions. A special split of the source terms allows us to design specific approximations such that the resulting WENO schemes satisfy the exact C-property for still water stationary solutions, and at the same time maintain their original high order accuracy and essentially nonoscillatory property for general solutions. Extensive numerical examples are given to demonstrate the exact C-property, accuracy, and nonoscillatory shock resolution of the proposed numerical method. The approach is quite general and can be adapted to high order finite volume and discontinuous Galerkin finite element methods on arbitrary triangulations, which constitutes an ongoing work.

References

- [1] D.S. Balsara, C.-W. Shu, Monotonicity preserving weighted essentially non-oscillatory schemes with increasingly high order of accuracy, *Journal of Computational Physics* 160 (2000) 405–452.
- [2] A. Bermudez, M.E. Vazquez, Upwind methods for hyperbolic conservation laws with source terms, *Computers and Fluids* 23 (1994) 1049–1071.
- [3] N. Crnjaric-Zic, S. Vukovic, L. Sopta, Balanced finite volume WENO and central WENO schemes for the shallow water and the open-channel flow equations, *Journal of Computational Physics* 200 (2004) 512–548.
- [4] F. Filbet, C.-W. Shu, Approximation of hyperbolic models for chemosensitive movement, *SIAM Journal on Scientific Computing*, submitted for publication.
- [5] N. Goutal, F. Maurel, Proceedings of the Second Workshop on Dam-Break Wave Simulation, Technical Report HE-43/97/016/A, Electricité de France, Département Laboratoire National d'Hydraulique, Groupe Hydraulique Fluviale, 1997.
- [6] J.M. Greenberg, A.Y. LeRoux, A well-balanced scheme for the numerical processing of source terms in hyperbolic equations, *SIAM Journal on Numerical Analysis* 33 (1996) 1–16.
- [7] A. Harten, P.D. Lax, B. Van Leer, On upstream differencing and Godunov-type schemes for hyperbolic conservation laws, *SIAM Review* 25 (1983) 35–61.
- [8] M.E. Hubbard, P. Garcia-Navarro, Flux difference splitting and the balancing of source terms and flux gradients, *Journal of Computational Physics* 165 (2000) 89–125.
- [9] G. Jiang, C.-W. Shu, Efficient implementation of weighted ENO schemes, *Journal of Computational Physics* 126 (1996) 202–228.
- [10] S. Jin, A steady-state capturing method for hyperbolic systems with geometrical source terms, *Mathematical Modelling and Numerical Analysis (M²AN)* 35 (2001) 631–645.
- [11] A. Kurganov, D. Levy, Central-upwind schemes for the Saint-Venant system, *Mathematical Modelling and Numerical Analysis* 36 (2002) 397–425.
- [12] R.J. LeVeque, Balancing source terms and flux gradients on high-resolution Godunov methods: the quasi-steady wave-propagation algorithm, *Journal of Computational Physics* 146 (1998) 346–365.
- [13] X.-D. Liu, S. Osher, T. Chan, Weighted essentially nonoscillatory schemes, *Journal of Computational Physics* 115 (1994) 200–212.
- [14] T.C. Rebollo, A.D. Delgado, E.D.F. Nieto, A family of stable numerical solvers for the shallow water equations with source terms, *Computer Methods in Applied Mechanics and Engineering* 192 (2003) 203–225.
- [15] P.L. Roe, Approximate Riemann solvers, parameter vectors, and difference schemes, *Journal of Computational Physics* 43 (1981) 357–372.
- [16] G. Russo, Central schemes for balance laws, in: Proceedings of the VIII International Conference on Nonlinear Hyperbolic Problems, Magdeburg, 2000.
- [17] C.-W. Shu, Essentially non-oscillatory and weighted essentially non-oscillatory schemes for hyperbolic conservation laws, in: B. Cockburn, C. Johnson, C.-W. Shu, E. Tadmor (Ed.: A. Quarteroni) *Advanced Numerical Approximation of Nonlinear Hyperbolic Equations*, Lecture Notes in Mathematics, vol. 1697, Springer, 1998, pp. 325–432.

- [18] C.-W. Shu, S. Osher, Efficient implementation of essentially non-oscillatory shock-capturing schemes, *Journal of Computational Physics* 77 (1988) 439–471.
- [19] C.-W. Shu, S. Osher, Efficient implementation of essentially non-oscillatory shock-capturing schemes, II, *Journal of Computational Physics* 83 (1989) 32–78.
- [20] M.E. Vazquez-Cendon, Improved treatment of source terms in upwind schemes for the shallow water equations in channels with irregular geometry, *Journal of Computational Physics* 148 (1999) 497–526.
- [21] S. Vukovic, L. Sopta, ENO and WENO schemes with the exact conservation property for one-dimensional shallow water equations, *Journal of Computational Physics* 179 (2002) 593–621.
- [22] S. Vukovic, N. Crnjacic-Zic, L. Sopta, WENO schemes for balance laws with spatially varying flux, *Journal of Computational Physics* 199 (2004) 87–109.
- [23] K. Xu, A well-balanced gas-kinetic scheme for the shallow-water equations with source terms, *Journal of Computational Physics* 178 (2002) 533–562.
- [24] J.G. Zhou, D.M. Causon, C.G. Mingham, D.M. Ingram, The surface gradient method for the treatment of source terms in the shallow-water equations, *Journal of Computational Physics* 168 (2001) 1–25.